

## Enhancing the processability and performance of polylactic acid resins

Emilia Garofalo, Paola Scarfato, Luciano Di Maio, and Loredana Incarnato

*An in-depth study of polylactide nanocomposite molecular characteristics demonstrates that selecting appropriate organoclays for each polylactide grade is a key issue.*

Poly(lactic acid) (PLA) is one of the most promising renewable and biodegradable polymers. The building block of PLA, i.e., 2-hydroxy propionic acid, can exist as either optically active D- or L-enantiomers. Depending on the proportion of these enantiomers, PLA with variable material properties can be derived. A wide spectrum of PLA polymers can thus be produced to match particular performance requirements. Properties such as high gloss and clarity, high tensile strength, good heat sealability, and a low coefficient of friction make PLA a suitable candidate for a wide variety of applications. There are, however, some issues, including low drawability, absent or weak strain hardening behavior, unsatisfactory toughness, and limited gas barrier properties, that need to be properly overcome.<sup>1</sup>

Recently, there have been several attempts to broaden the processability and the end-use properties of PLA, through the development of PLA/clay nanocomposites.<sup>2–5</sup> Substantial progress has been made in the analysis of the many relationships that exist between the system composition, processability, and morphology of the polylactide-silicate nanocomposites. A general understanding, however, has yet to emerge. Additional theoretical and experimental studies are therefore required for the proper selection of the best organoclays for well-specified PLA grades and processing technologies.

In this work, we prepared PLA nanocomposites—reinforced with commercially available organoclays—with the use of a melt intercalation technique. We selected two montmorillonites—Cloisite 30B (C30B) and Nanofil SE3010 (NSE3010)—as the nanofillers. These layered silicates are characterized by having different organic modifiers that provide a more pronounced polar character in C30B and a higher basal interlayer spacing for NSE3010 (see Table 1). The resins that we used for the polymer matrices were two grades of semi-crystalline PLA (PLA 4032D and PLA 2003D) that contain different amounts of the

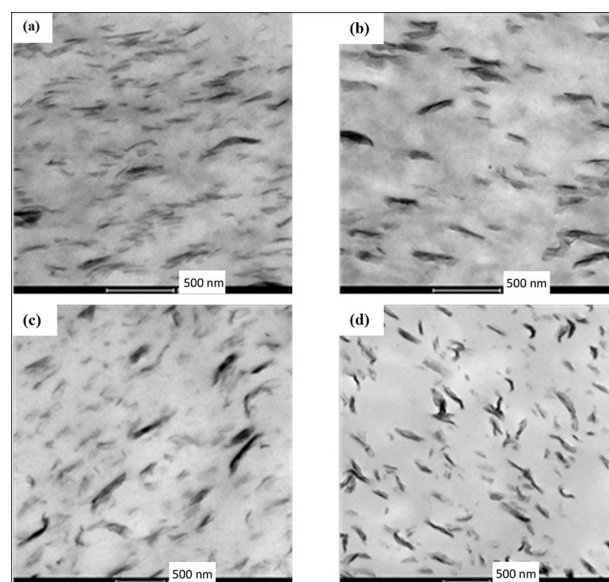


**Figure 1.** Transmission electron microscope images of polylactic acid (PLA) nanocomposite samples. Two different grades of semi-crystalline PLA (PLA 4032D and PLA 2003D) are used for the polymer matrix, and two montmorillonites—Cloisite 30B (C30B) and Nanofil SE3010 (NSE3010)—act as the nanofillers. (a) PLA 4032D+C30B, (b) PLA 4032D+NSE3010, (c) PLA 2003D+C30B, and (d) PLA 2003D+NSE3010.

D-isomer (1.5 and 4%, respectively). We have also conducted an in-depth investigation of the molecular characteristics of the neat PLA resins,<sup>6</sup> and found a high-molecular-weight tail in the PLA 2003D resin.

To directly investigate the silicate distribution/dispersion within our hybrids, relative to the system's bulk composition, we obtained transmission electron microscope (TEM) images for all the melt-compounded samples. For the case of the PLA4032D-based nanocomposites—see Figure 1(a) and (b)—we observe a higher degree

*Continued on next page*

**Table 1.** Chemical structure and basal interlayer spacing ( $d_{001}$ ) of the organic modifiers for each organoclay. C: Carbon. H: Hydrogen. N: Nitrogen. T: Tallow (i.e., about 65% C18, about 30% C16, and about 5% C14).

Organoclay	$d_{001}$ [Å]	Organic modifier
Cloisite 30B (C30B)	18.5	$\begin{array}{c} \text{CH}_2\text{CH}_2\text{OH} \\   \\ \text{CH}_3 - \text{N}^+ - \text{T} \\   \\ \text{CH}_2\text{CH}_2\text{OH} \end{array}$
Nanofil SE3010 (NSE3010)	36.0	$\begin{array}{c} \text{CH}_3 \\   \\ \text{H}_3\text{C} - \text{N}^+ - \text{HT} \\   \\ \text{HT} \end{array}$

of silicate dispersion with smaller stacks of the intercalated filler for the C30B hybrid system. For the PLA2003D-based nanocomposite samples, however, we find slight differences between the samples. For instance, as shown in Figure 1(c) and (d), there is a more uniform size distribution of the silicate particles for the PLA2003D+NSE3010 system.

We have also conducted rheological measurements, in shear and elongational mode, on all of our samples. Our results indicate that the rheological response of the nanocomposite systems is correlated to the nanostructure that is obtained and to the different polymer–clay affinities. The complex viscosity ( $\eta^*$ ) measurements of the neat PLA resins and their nanocomposite samples (i.e., containing C30B and NSE3010 organoclays) are plotted in Figure 2 as a function of angular frequency.

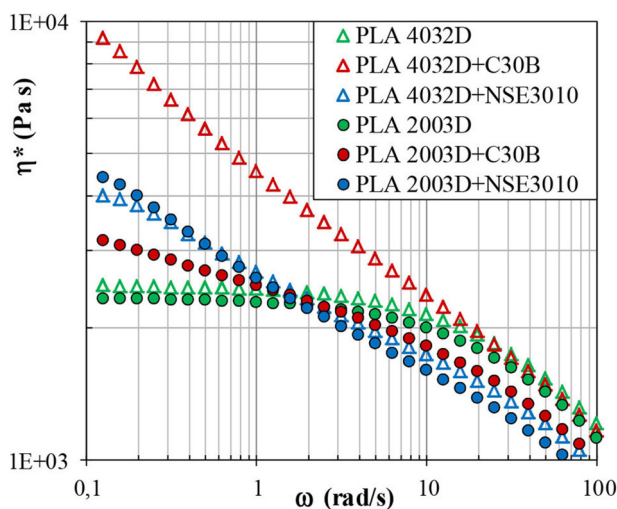


**Figure 2.** Complex viscosity ( $\eta^*$ ), as a function of angular frequency ( $\omega$ ), for the neat PLA matrices and their nanocomposites. Measurements were obtained at a temperature of 190°C.

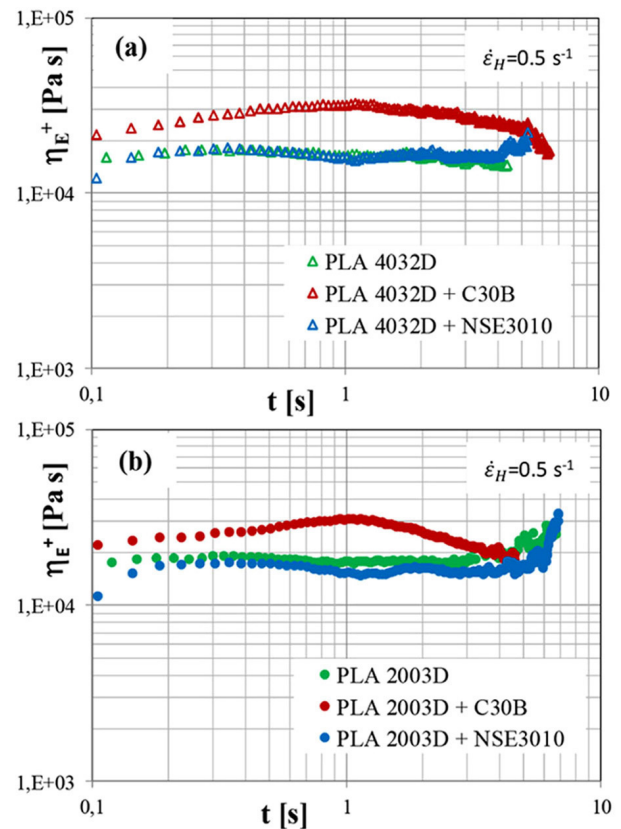


**Figure 3.** Elongational viscosity ( $\eta_E^+$ ) data shown as a function of time ( $t$ ). These measurements were obtained at a temperature of 180°C and a Hencky strain rate ( $\dot{\epsilon}_H$ ) of  $0.5\text{s}^{-1}$  for (a) the neat PLA 4032D matrix and its nanocomposites, and (b) the neat PLA 2003D matrix and its nanocomposites.

For the PLA 4032D-based hybrid systems, the C30B nanoclay produces the greatest increases in  $\eta^*$  and more pronounced shear thinning behavior, over the whole range of analyzed frequencies, whereas for the PLA 2003D-based hybrid systems, the NSE3010 sample exhibits stronger shear thinning behavior at low frequencies with respect to the C30B sample. We believe that the presence of two hydroxyl (OH) groups in the C30B structure promotes an affinity with the carbon–oxygen double bonds that are present in the PLA backbone, and thus cause polymer intercalation to be favored. Alternatively, the presence of the high-molecular-weight tail in the PLA 2003D resin could cause a reduction in the diffusion of the macromolecular chains between the silicate layers. In particular, C30B has half the basal interlayer spacing of NSE3010 (see Table 1). Intercalation of PLA 2003D chains inside the layers of C30B is therefore much more difficult than for NSE3010.

The material response to extensional deformations is also of great interest in many important polymer processing operations. We have thus analyzed the effect of the system composition (i.e., PLA grade and organoclay type) on the elongational rheological behavior of the nanocomposites. The elongational viscosity curves (at a Hencky strain rate of  $0.5\text{s}^{-1}$ ) for our PLA nanocomposites are illustrated in Figure 3. We find that the NSE3010-based hybrids have viscosities that are similar to the neat matrices in the linear region. They also exhibit a strain hardening behavior in this region over long periods. This peculiar extensional thickening behavior may be related to the presence of the silicate platelets. These build up in three-dimensional arrangements and hinder extensional flow (in a manner similar to branches of macromolecular chains). In other words, for hybrid systems that are characterized by low polymer–clay affinities (e.g., the NSE3010-based nanocomposites), uniaxial elongational flow seems to promote edge-to-face electrostatic interactions between silicate platelets. Such behavior is also observed in other systems.<sup>7–9</sup> In contrast, the C30B nanocomposites exhibit extensional viscosity values that are higher than the neat polymers and have no strain hardening behavior. In these cases, the strong polymer–clay affinities of the C30B and the PLA resins shield the electrostatic clay–clay interactions, which are responsible for the strain-hardening phenomenon. This means that at high Hencky strains, the alignment of the silicate layers toward the stretching direction is favored (i.e., a consequence of the alignment of the polymer chains).

The results of our work demonstrate that even small differences in the molecular structure of a polylactide resin—and the addition of clays with different organomodifiers—can affect the nanomorphology that develops and the processability of the nanocomposite. Moreover, the structural modifications that are induced by stretching in PLA nanocomposites strongly influence properties such as extensional viscosity and strain hardening behavior. These properties are fundamental for assessing the performance of the nanocomposites in processing operations, especially where extensional flow is mainly involved. These modifications are highly dependent on the polymer–clay affinity of the system. In our future work we will assess and optimize the processing conditions for cast and blown film extrusion of PLA 4032D+C30B and PLA 2003D+NSE3010 nanocomposite systems, respectively.

## Author Information

**Emilia Garofalo, Paola Scarfato, Luciano Di Maio, and Loredana Incarnato**

Department of Industrial Engineering  
University of Salerno  
Fisciano, Italy

Emilia Garofalo is a research fellow. Her research activity is focused on the study of the processing–structure–properties relationship of polymer nanocomposites.

Paola Scarfato is an associate professor of materials science and technology. Her current research focuses on the development, functionalization, and characterization of novel polymer materials, as well as on the development of micro- and nanosized functional systems.

Luciano Di Maio is an associate professor of materials science and technology. His research areas involve thermoplastic polymer processing, including the preparation and characterization of polymer composites and nanocomposites.

Loredana Incarnato is a full professor of materials science and technology. Her research activity is focused on the rheology and processing of polymers and polymer nanocomposites, polymer recycling, as well as biodegradable and active polymeric systems for food packaging applications.

## References

1. L.-T. Lim, R. Auras, and M. Rubino, *Processing technologies for poly(lactic acid)*, **Prog. Polym. Sci.** **33**, pp. 820–852, 2008.
2. A. K. Mohapatra, S. Mohanty, and S. K. Nayak, *Effect of PEG on PLA/PEG blend and its nanocomposites: a study of thermo-mechanical and morphological characterization*, **Polym. Compos.** **35**, pp. 283–293, 2014.
3. J.-M. Raquez, Y. Habibi, M. Murariu, and P. Dubois, *Poly(lactide) (PLA)-based nanocomposites*, **Prog. Polym. Sci.** **38**, pp. 1504–1542, 2013.
4. L. Di Maio, P. Scarfato, M. R. Milana, R. Feliciani, M. Denaro, G. Padula, and L. Incarnato, *Bionanocomposite poly(lactic acid)/organoclay films: functional properties and measurement of total and lactic acid specific migration*, **Packag. Technol. Sci.** **27**, pp. 535–547, 2014.
5. E. Garofalo, P. Scarfato, L. Di Maio, and L. Incarnato, *Effect of nanocomposite composition on shear and elongational rheological behavior of PLA/MMT hybrids*, **AIP Conf. Proc.** **1599**, pp. 422–425, 2014.
6. L. Di Maio, E. Garofalo, P. Scarfato, and L. Incarnato, *Effect of polymer/organoclay composition on morphology and rheological properties of poly(lactide) nanocomposites*, **Polym. Compos.** **36**, pp. 1135–1144, 2015.
7. E. Garofalo, M. L. Fariello, L. Di Maio, and L. Incarnato, *Effect of biaxial drawing on morphology and properties of copolyamide nanocomposites produced by film blowing*, **Euro. Polym. J.** **49**, pp. 80–89, 2013.
8. E. Garofalo, G. M. Russo, P. Scarfato, and L. Incarnato, *Nanostructural modifications of polyamide/MMT hybrids under isothermal and nonisothermal elongational flow*, **J. Polym. Sci., Part B Polym. Phys.** **47**, pp. 981–993, 2009.
9. E. Garofalo, G. M. Russo, L. Di Maio, and L. Incarnato, *Study on the effect of uniaxial elongational flow on polyamide based nanocomposites*, **Macromol. Symp.** **247**, pp. 110–119, 2007.